Thomas, B.G. and W. R. Storkman, "Mathematical Models of Continuous Slab Casting to Optimize Mold Taper", *Modeling and Control of Casting and Welding Processes - IV*, Palm Coast, FL, April 17-22, 1988, AF Giamei and GJ Abbaschian, eds., The Metallurgical Society, Warrendale, PA, 1988, pp. 287 - 297.

# MATHEMATICAL MODELS OF CONTINUOUS SLAB CASTING

# TO OPTIMIZE MOLD TAPER

B. G. Thomas and W. R. Storkman

Department of Mechanical and Industrial Engineering
University of Illinois at Urbana-Champaign
1206 West Green Street
Urbana, IL 61801

## Abstract

The behavior of the shell during early stages of solidification in the mold is very important to the ultimate quality of continuously cast steel. To further understand this behavior, two-dimensional, transient finite-element models have been developed to simulate heat flow, shrinkage, and stress generation in the solidifying steel shell in the mold region of a continuous slab casting machine. The models are applied to explore the influence of mold taper, particularly along the narrow face, on heat flow and shell development. These calculations indicate that the constant taper presently used on the narrow face mold walls is inadequate. The combination of bulging (where the taper is too little) and compression (where the taper is too great) can distort the shell, leading to defects such as off-corner surface depressions in stainless slabs, and even longitudinal cracks in other grades. The mathematical models are then used to explore alternate taper designs that should reduce or eliminate this problem.

## Introduction

The formation of defects in continuously cast steel slabs is determined greatly by the behavior of the thin, growing shell during the early stages of solidification in the mold [1]. During this time, the shell shrinks away from the mold due to thermal contraction, and a gap is formed between the mold and the strand. This causes the rate of heat flow from the strand to diminish dramatically, particularly near the corner. The extent of this gap depends on the strength of the thin shell to withstand the ferrostatic pressure pushing it outward, the casting speed, the casting powder heat transfer characteristics, and the amount of mold taper present to offset the shrinkage. With improper taper, the combination of bulging (where there is too little taper) and compression (where there is too much taper) may distort the shell and even form cracks or breakouts while it is weak and possibly fragile.

Stainless steel slabs are plagued by 2-5mm depressions or "gutters" that form just off the corner along the wide face of the slab, as pictured in Figure 1. They are accompanied by bulging along the narrow face. This is a problem because subsequent reheating operations require the surface to be ground flat. In plain carbon steel castings, this location often exhibits cracks as well. The present research uses mathematical models to simulate temperature and stress development in the solidifying shell and focuses on the influence of mold taper on heat transfer and deformation of the shell in the critical corner region. The ultimate goal of the project is to increase understanding of the mechanism of formation of these defects, and to (hopefully) find a taper design for the narrow face of the mold that more closely matches the natural shrinkage of the shell, in order to reduce stress and distortion and their related problems.

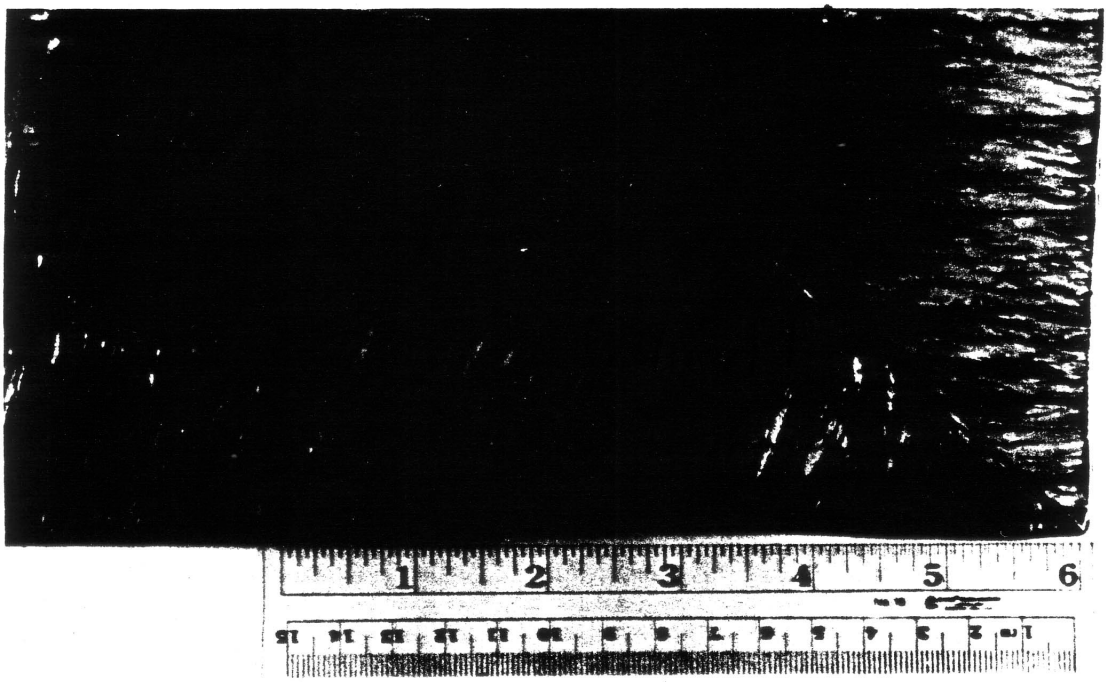


Figure 1 - Photograph of corner section of 304 stainless-steel slab showing off-corner depression

## Model Description

Although the continuous casting process has been modelled extensively, only a few previous models have considered stress generation in slab casting machines [1]. Due to the complexity of the problem, none has incorporated all of the known physical and mechanical phenomena that govern deformation of the shell during the critical early stages of solidification in the mold. The present work attempts to incorporate most of those phenomena that are believed to be important to the formation of off-corner depressions and cracks, into a thermal stress model of a continuously-cast slab during solidification in the mold. This includes the coupling together of separate two-dimensional, transient, models for heat flow and stress generation, to track the behavior of a transverse slice through the slab as it moves down through the caster. It also includes both ferrostatic pressure and the resisting force from the mold walls.

The models are based on previously developed models for temperature and stress development in static-cast ingots [2,3]. A brief description of the salient and additional features of each model will now be given, followed by a description of the coupling procedure.

### Heat Flow Model

Because the depression defect is primarily longitudinal and exhibits two-fold symmetry, only one quarter of a transverse, section through the slab was considered. The transient, two dimensional heat conduction equation was solved using the finite element method over the domain shown in Figure 2. The two-fold symmetry is imposed mathematically by setting heat flow through the slab centerlines to zero.

Extensive testing using analytical solutions from 3 different solidification problems determined that the heat flow model can most accurately calculate temperature histories for this type of problem using the DuPont time stepping technique with a consistent formulation of the capacitance matrix. The optimum

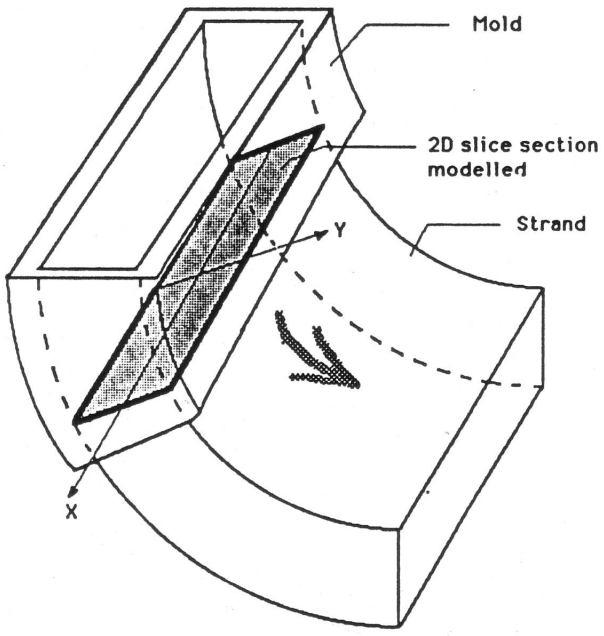


Figure 2 - a) Schematic of slab caster showing transverse section simulation domain

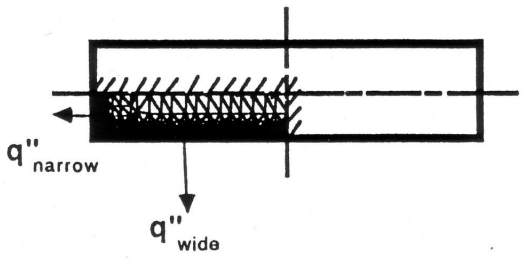


Figure 2 - b) Slab section showing mesh and boundary conditions

time step size was found to be approximated by $\Delta t = (0.3)(\Delta x^2)/\alpha$, where $\Delta t$ is the time step size, $\Delta x$ is the smallest distance across an element in the direction of the heat flow, and $\alpha$ is the thermal diffusivity of the solidifying steel. Further details regarding the formulation, solution technique, and analytical verification of the model can be found elsewhere [4].

The model presently accounts for convection in the liquid pool by simply increasing the effective thermal conductivity for molten steel. However, it is well-known that steel flowing from a bifurcated nozzle impinges the narrow face with a maximum heat input at a location very low in the mold [5]. This phenomenon is being investigated separately using a different finite element model [6]. Eventually, it is planned to use the output from this model as the boundary condition for heat flux to the solid/liquid interface of the present model, to take this effect into account.

Interfacial Gap Heat Conduction Model

Heat transfer out of the wide and narrow faces of the strand, across the interfacial gap that forms between the shell and the mold, is calculated as a time- and position-dependent function. This function depends on the mold and strand surface temperatures and the thickness of the gap. The strand surface temperature is based on model calculations at the previous time step and mold temperatures are stored in a file as a function of distance down the caster. The thickness of the gap is calculated knowing the position of the strand surface, calculated by the stress model at the previous time step, and the position of the mold wall at a given location and time. Positions of the mold wall, and corresponding surface temperatures, can be determined from previous runs of a steady-state thermal-stress model of the mold itself, assuming typical values for the input heat flux boundary condition.

Initial runs of the model determined that the results are quite sensitive to the gap heat transfer function employed. In fact, the shell thickness, distorted shape, and extent of hot spot formation can be made to vary greatly with minor changes to this function. Thus, an effort was made to develop a reasonable model of heat flow across the gap.

The function presently employed involves a system of five resistances to heat conduction, shown in Figure 3b. Heat can either radiate through the semi-transparent flux, or conduct through a series of four resistances, consisting of two contact resistances and two thickness/conductivity resistances. The total heat flux is then characterized by the contact resistances to heat flow at both the flux/mold and flux/strand interfaces, the thermal conductivities of the two materials assumed to fill the gap (molten casting powder and air/gas vapor), the minimum and maximum powder thicknesses, the effective emissivity, temperature variations of the two surfaces, and the calculated total size of the gap.

Values for the thermal properties and flux thicknesses were chosen to be consistent with experimentally reported values, (eg. ref. [7]). The contact resistances were chosen to match experimentally derived heat flux curves, which are governed primarily by heat flow to the wide face where ferrostatic pressure maintains a relatively small interfacial gap size.

The rationale for this model is illustrated in Figure 3a. It assumes that a minimum thickness gap exists, even at the meniscus, which is filled with highly conductive (1.5 W/mK), molten powder flux. This minimum thickness, currently set at 0.05mm, should be dependent on the powder viscosity, its melting rate, and the casting speed used. The molten powder is then assumed to flow to fill the gap until it cools and becomes too viscous, characterized by the "maximum powder

thickness." (currently 0.1mm). All further expansion of the gap is filled with lower conductivity material (0.10 W/mK), consisting primarily of air and other gases.

Sensitivity Analysis. Initial runs of the model have determined that the most important factor influencing heat flow across the gap along the wide face is the values of the contact resistances employed. This is because the gap itself is too small for the conductivity of the material filling it to be important. At the flux/mold interface, a contact resistance of 1/3000 $W/m^2K$ is currently employed. This results in peak heat flux calculations at the meniscus that match experimentally measured values, and is consistent with values of perfect contact resistances used previously. At the flux/strand interface, the contact resistance increases from zero, when both materials are fluid, to 1/4000 $W/m^2K$ when the steel becomes solid (1399 °C), to 1/1200 $W/m^2K$ when the flux becomes solid (1140 °C).

Along the narrow face, and in the corner region, the most critical factor influencing heat flow is the size of the gap, as expected. Model runs also determined that the results are relatively insensitive to the previously calculated mold distortion values, since these are very small. Although the mold itself expands a significant amount, (reaching a maximum deflection of almost 0.5mm at the center of the wide face), the gap depends only on the *difference* between values of this expansion at the meniscus and other locations down the mold face. Typical runs of the steady-state thermal stress analysis of the mold found this difference to be on the order of only 0.01mm [8]. This is contrary to experience in billet casting molds, which have thinner walls integrated into one piece, and more significant differential expansions are found [9].

Radiation and radiation-conduction provide a relatively small fraction of the total heat transferred across the gap where the gap is small, such as found along the wide face. Thus, large changes in the effective emissivity, $\varepsilon$, produced little change in the results. Currently, $\varepsilon$ is set=0.7. Radiation does grow in importance as the gap size increases, but only reaches 50% of the total heat transferred when the gap size exceeds 0.5mm.

Verification. An indication of the accuracy of this model for heat flow across the gap, and the gap calculations from the stress model, is shown by a comparison of the calculated total heat flux removed from the slab with experimental measurements. Such a comparison is given in Figure 4, which shows reasonable agreement with measurements from Samarasekera [10] that were performed on the the slab caster being simulated.

Stress Model

An incremental, two-dimensional, transient, elasto-visco-plastic, thermal stress model was used to determine the internal stress state in the shell arising from the changing temperature gradients calculated by the heat-flow model. The model evaluates increments of plastic strain at each time step using a plastic strain rate function, determined separately, that is transformed into vector components using the Prandtl-Reuss plastic flow equations and the Von Mises yield criterion. Load increments from the thermal strain are calculated from the temperatures generated by the heat flow model at successive time steps, using an input function for the thermal linear expansion. The basic formulation of the model and solution procedure has been given previously [3].

The model has been modified in several ways for the slab casting problem. It can now handle either plane stress or generalized plane strain conditions, although the latter requires iteration within a time step. The heat flow and stress models are "stepwise coup-led", as the solution alternates between the thermal and stress calculations as the slice moves down through the mold in successive time steps. This approach has been used in previous recent models [11].

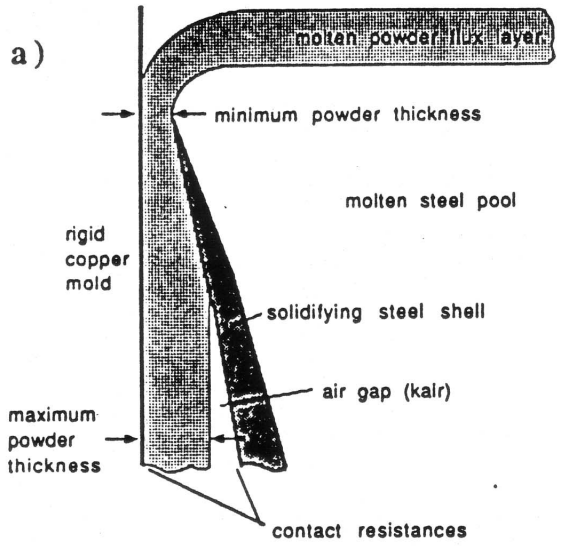


Figure 3 - Calculation of heat transfer across the interfacial gap

a) Idealized representation of gap region
b) Schematic of resistance model employed

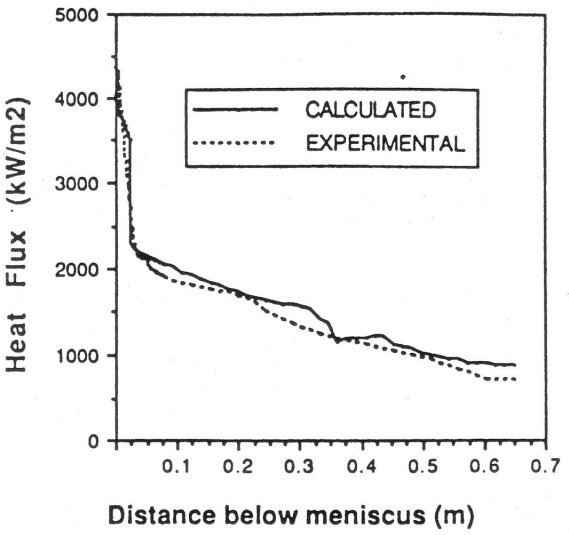


Figure 4 - Comparison of calculated and measured [9] heat flux down the mold

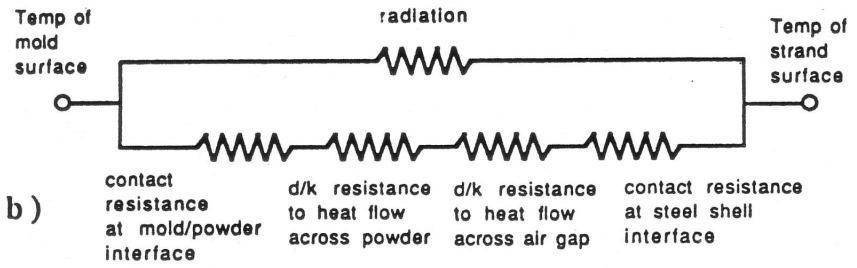


The model uses the same mesh of 3 node triangular elements employed in the thermal analysis. Ferrostatic pressure is applied to the two nodes of every "mushy" element that has exactly two nodes below the solidus and one node above. The incremental pressure load is proportional to the density, casting speed and time step size. It is applied in the direction of decreasing temperature, as determined by the third node in the element.

A temperature-dependent function for the elastic modulus is employed which reduces E from 80 GPa at 1360 °C in 2 linear stages by multiplying E by a factor which varied from 1 at 40 °C below the solidus to 0.1 at 0.3 fraction liquid to 0.01 at the liquidus. Stress generation in the liquid is suppressed simply by lowering the elastic modulus to 1 MPa in liquid elements.

Iteration is performed within each time step to converge on as many as four separate variables: the application of mold restraining gap elements, the size of the gaps calculated by the stress model (compared with those assumed by the heat flow model), the plastic strain rates (which both depend on and affect, the current stress state), and the value of strain in the z direction, (for generalized plane strain calculations). Due to convergence difficulties encountered when plasticity and generalized plane strain are present, simulations are currently being run assuming an elastic, plane stress condition.

To account for the restraining effect of the mold on the thin shell, deforming in the presence of internal ferrostatic pressure, gap elements are created between nodes on the surface of the solidifying shell and the mold wall.

The position of nodes on the mold wall are specified as a function of the desired input mold taper, and previous distortion data. To restrain only those nodes that attempt to move through the mold wall, the stiffness of these gap elements is set either to zero (ie not applied) or to a value that is five orders of magnitude higher than the stiffness of the corner node (the coldest, stiffest node). Since it is equally important not to restrain nodes that wish to shrink away from the mold wall, iteration is required within each step to determine the proper settings of the gap stiffnesses. This is accomplished by solving for displacements, first assuming that no nodes violate the mold wall. The stress calculations at this time step are then repeated, with the high stiffness restraint applied to all nodes that attempted to move into the mold by more than a set tolerance (currently 0.005mm). Again, the location of each node on the strand surface is compared to the corresponding position of the mold wall. If any "restrained" nodes lie outside the mold wall (indicating their desire to shrink) or if more than 6 nodes lie inside the mold by more than the tolerance, then another iteration is required. Iteration is continued until both conditions are satisfied, which usually requires 3-8 steps.

Similar iteration procedures are required for convergence on the plastic strain rates, at the beginning and end of each time step, and on strain in the out-of-plane z direction for generalized plane strain simulations.

After the gap element conditions, plastic convergence criteria, and z direction strain criterion (for generalized plane strain simulations) have all been satisfied, the displacements at the boundary, which determine the gap, are compared against those used for the heat transfer calculations at that time step. These displacements must agree within 10% before the stress, strain, and displacement increments are added to the accumulated totals, and the solution can proceed to the next step. If not, gaps are recalculated from the previous and current values using a relaxation factor of 0.4, and the entire process of calculating temperatures in the heat flow model, and iterating in the stress model until the incremental displacements satisfy all convergence criteria, is repeated. This procedure is repeated until convergence is satisfied. A typical run of the elastic model takes about 20 minutes on the Cray X/MP supercomputer.

## Results and Discussion

The input conditions used in the simulations are given in Table I. Caster geometry and process variables were taken for AISI 304 stainless steel slabs at the Armco Butler plant [12]. The calculated temperature distribution in the shell at various times during cooling in the mold is presented in Figure 5, along with the corresponding distorted shape, which is shown magnified 30 times.

This simulation was performed using an "ideal" taper along the narrow face, after 5s of cooling. This was accomplished by matching the mold wall position to the center of the narrow face (allowing for the 0.5mm minimum powder thickness). It thus allows the narrow face to shrink as it pleases (after first solidifying against a resisting wall) with heat transfer behaving as if a fortuitous continuous taper had been employed along the narrow face. This provides insight into how the narrow face would behave.

The results show a reasonable temperature distribution with an average shell thickness at mold exit that is close to the 12mm thickness commonly found in breakout shell measurements for this caster [12]. The interesting feature of Figure 5 is the slight depression found just off the corner of the slab at 5 and 10s. This phenomenon is due to rotation of the corner as the ferrostatic pressure pushes against the mid-narrowface and corresponds with a "hot spot" at the same location. The depression disappears by the time the slab exits the mold.

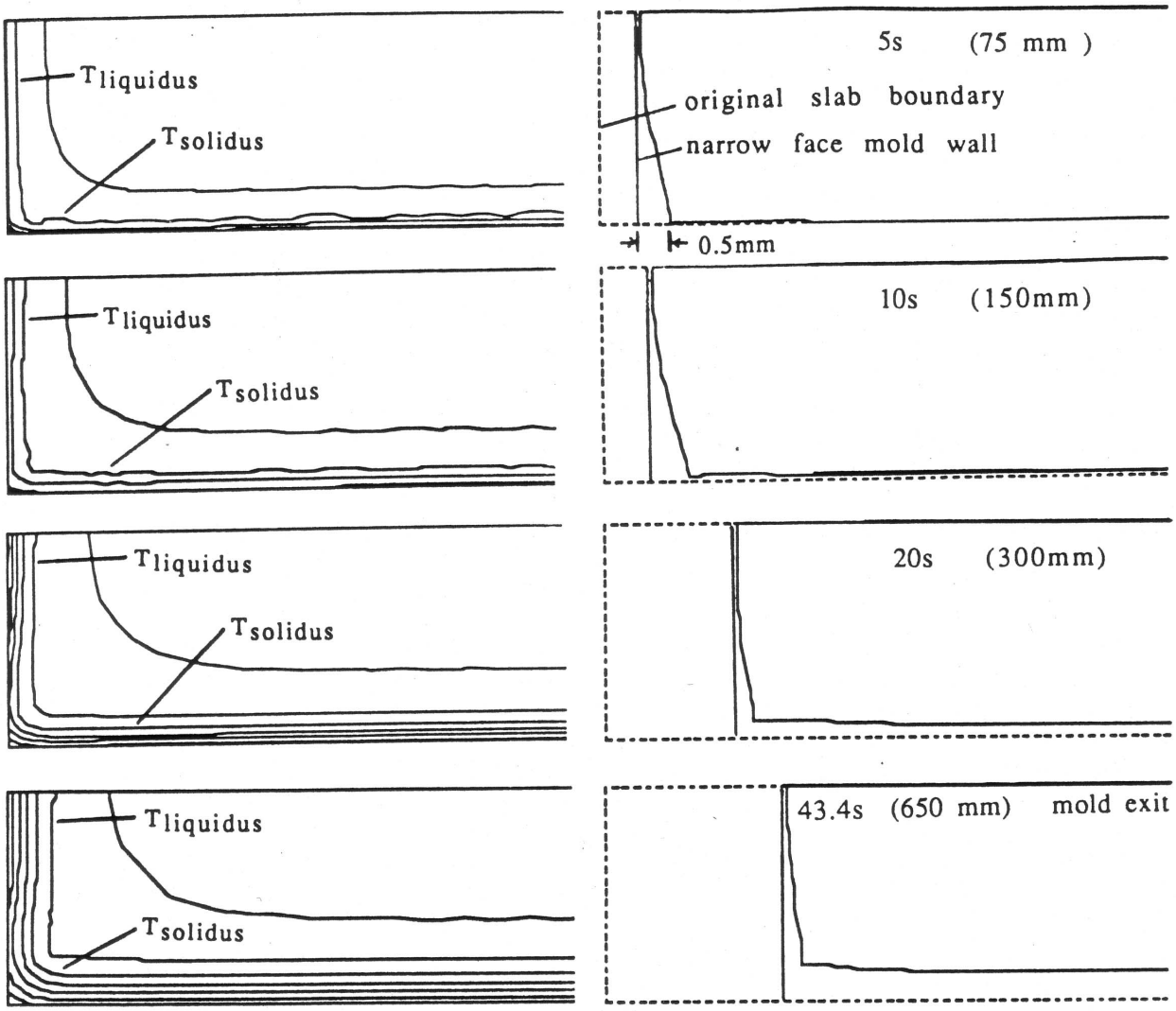


Figure 5 - Calculated temperature contours (°C) and corresponding distorted slab shape (magnified 30X) at various times in the mold (using "ideal taper" along the narrow face)

Using a straight, linear taper along the narrow face results in the formation of more severe hot spots in the off-corner regions, as shown in Figure 6. These are the result of reduced heat flow across the large corner gap without the benefit of 2D heat flow found at the corner itself. The thinning of the shell that accompanies the hot spot on the wide face may be an important factor in the formation of defects, including off-corner gutters and breakouts.

Figure 7 presents a plot of shrinkage at the center and corner of the narrow for the ideal taper run. The 1.15%/m linear taper of the end plates, currently employed, is included for comparison. This figure shows that this linear taper is a fairly close approximation to how the narrow face desires to shrink. However, it allows formation of a large gap at the top of the mold, while at the bottom, the mold wall pushes against the shell. It is interesting to note that the extent of this non-linearity in narrow face shrinkage predicted using the two-dimensional, coupled model, is much less than that found with a simple, one-dimensional shrinkage calculation.

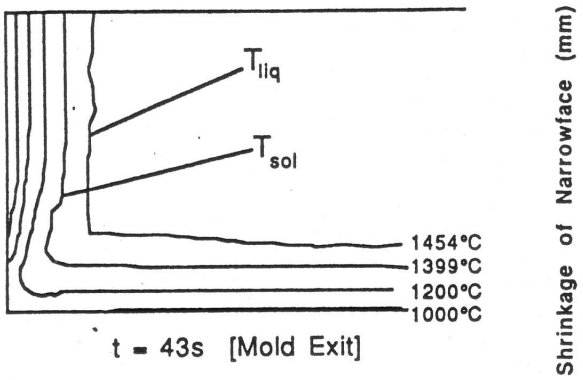


Figure 6 - Calculated temperature contours at mold exit (using straight, 1.15%/m taper along narrow face)

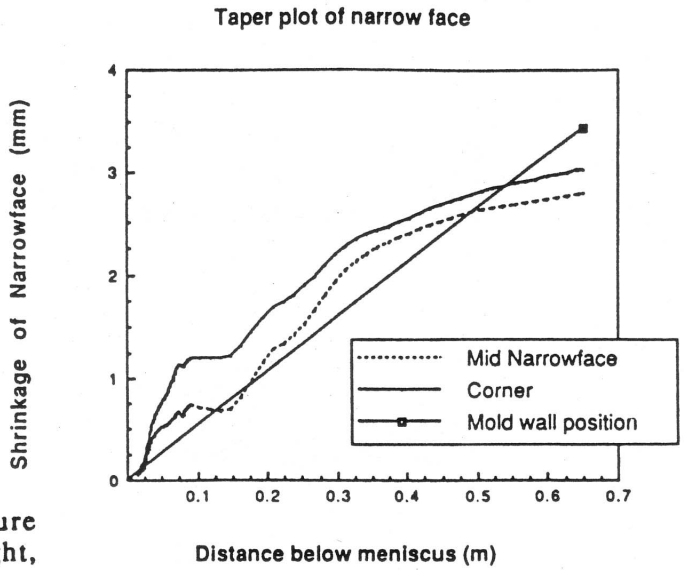


Figure 7 - Calculated position of narrow face (middle and corner) using "ideal taper", compared with actual wall position (assuming 1.15%/m taper)

## Mechanism of Surface Depression Formation

Figure 8 shows a proposed mechanism for the formation of off-corner surface depressions. The model results indicate that near the top of the mold, a simple linear taper cannot compensate for the rapid shrinkage of the wide face. While the wide face shrinks, the narrow face shell is held against the mold by ferrostatic pressure, so the shell opens up a relatively large air gap near the corner along the narrow face. This forces the narrow face shell to reheat near the corner. It also causes the shell to rotate slightly about the rigid solidified corner. This produces a slight depression close to the corner which results in reheating of the region adjacent to the corner region along the wide face as well. A mechanism similar to this is believed to be responsible for off-corner internal cracks in billets [13].

Further down the mold, wide face shrinkage is less and the linear taper forces the narrow face wall to impinge on the shell, producing a compressive stress in the shell along the wide face. If this compressive stress is high enough, the shell will buckle slightly at its weakest point, which is the thinned region off the corner of the wide face where the small depression is already present, and thus will enlarge the surface depression.

This mechanism has not, as yet, been fully verified by the model predictions. The relative importance of the two proposed steps is not known and there may be other factors as well, such as further narrow face bulging upon exit from the mold. However, the model now provides a tool which can be used to refine this mechanism and to evaluate solutions to the problem.

## Conclusion

Transient finite element models have been developed and verified to simulate heat flow, shrinkage, and stress generation in the solidifying steel shell of a continuously cast slab. A sensitivity analysis using the model suggests that the function describing heat transfer across the gap and the gap size are critical

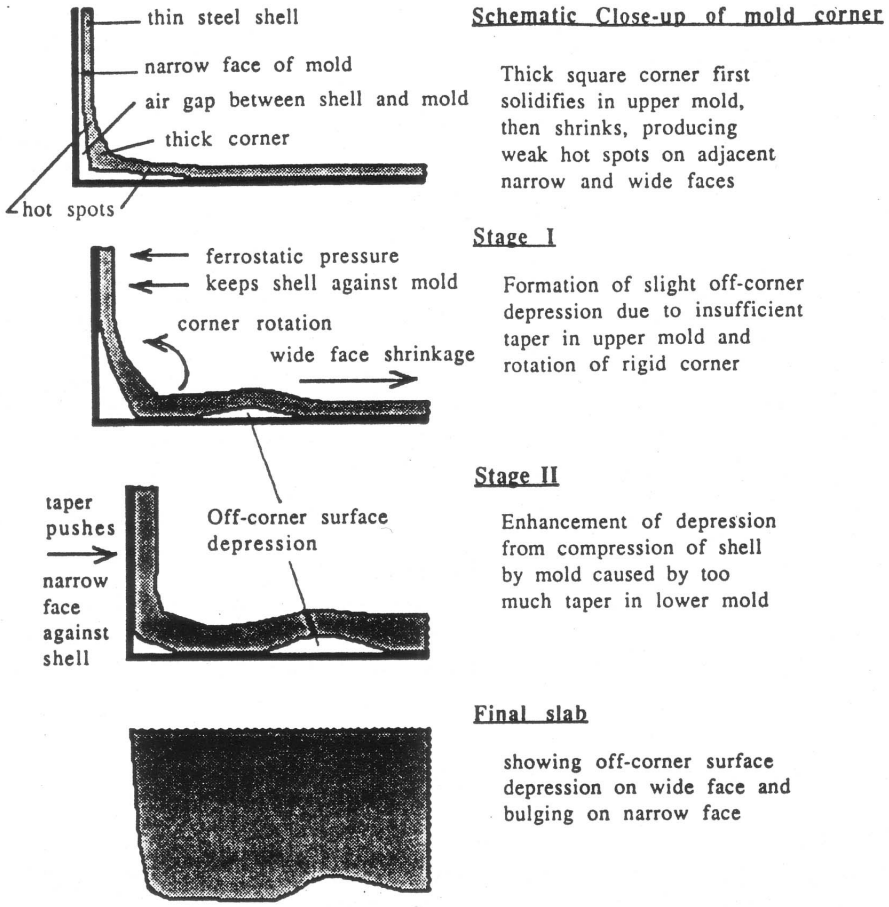


Figure 8 - Suggested mechanism of formation of off-corner surface depressions

to the accurate prediction of heat flow from the strand. The effect on hot spot development and slab shape of using a continuous taper along the narrow face, has been compared with that from a simple linear taper. Based on the model calculations, a mechanism has been proposed for the formation of off-corner surface depressions. Further enhancement and validation of the model and additional runs are required to refine these predictions in preparation for industrial trials using end plates designed with an optimized mold taper.

## References

1. A. Grill., K. Sorimachi, and J.K. Brimacombe, Met. Trans. B, Vol. 7B, 1976, pp.177-189.

2. B.G. Thomas, I.V. Samarasekera, and J.K. Brimacombe, Met. Trans. B., Vol. 18B, No. 1, 1987, pp119-130.

3. B.G. Thomas, I.V. Samarasekera, and J.K. Brimacombe, Met. Trans. B., Vol. 18B, No. 1, 1987, pp131-147.

4. B.G. Thomas, I.V. Samarasekera, and J.K. Brimacombe, Met. Trans. B, 1984, Vol. 15B, pp.307-318.

5. Nakato, H., M. Ozawa, K. Kinoshita, Y. Habu, and T. Emi, Trans. of the Iron and Steel Inst. Japan, Vol. 24, No. 11, 1984, pp. 957-965.

6. L. Mika and B.G. Thomas, Modelling of Casting and Welding Processes, to be presented at Eng. Found. conference in Palm Coast, Florida, April 17-22, 1988.

7. S. Ohmiya, K.-H. Tacke, and K. Schwerdtfeter, Ironmaking and Steelmaking, 1983, Vol. 10, No. 1, pp24-30.

8. B. G. Thomas, L. Mika, and J. Azzi, "Three-Dimensional Heat Flow and Stress Models of Continuous Casting of Steel Slabs", report submitted to Inland, Bethlehem, and Armco Steel, October, 1987.

9. J.E. Kelly, K. P. Michalek, B. G. Thomas, and J. A. Dantzig, Met. Trans. B, in print, 1988.

10. I.V. Samarasekera, and J.K. Brimacombe, Canadian Metallurgical Quarterly, 1979, Vol. 18, pp. 251-266.

11. J.O. Kristiansson, Journal of Thermal Stresses, Vol. 7, 1984, pp209-226.

12. G. Drigel, private communication, 1987.

13. R. Bommaraju, J.K. Brimacombe and I.V. Samarasekera, ISS Trans., Vol. 5, 1984, pp.95-105.

Table I. Standard Input Conditions for Model Runs

| | |
|---|---|
| Mold dimensions: | |
| Slab thickness | 203 mm |
| Slab width | 914 mm |
| Mold length | 700 mm |
| Taper | 1.0 %/m or "ideal" (narrow face)<br>0.77%/m (wide face) |
| Material properties: | |
| Grade | 304 Stainless steel<br>(18% Cr, 8% Ni, .06%C) |
| Phase | 100 % $\gamma$ |
| Liquidus temperature | 1454 °C |
| Solidus temperature | 1399 °C |
| Thermal expansion coefficient | 0.0021 %/°C |
| Density, $\rho$ | 8000 kg/m$^3$ |
| Thermal conductivity, k | temperature dependent [2] |
| Enthalpy, H | temperature dependent [2] |
| Elastic modulus | temperature dependent |
| Poisson Ratio | 0.3 |
| Casting conditions: | |
| Pouring temperature | 1485 °C |
| Casting speed | .015 m/s (0.9m/min) |
| Meniscus level | 50 mm below mold top |

## Acknowledgements

The authors wish to thank Armco Inc. both for a grant which made this research possible and for the provision of valuable data. In addition, valuable discussions with Gary Drigel of Armco, and Ismael Saucedo of Inland Steel are gratefully acknowledged. Thanks are also due to the National Center for Supercomputer Applications for time on the CRAY-XMP/48.